

RAP-SAM : Towards Real-Time All-Purpose Segment Anything

Shilin Xu^{1,4*} Haobo Yuan² Qingyu Shi¹ Lu Qi³ Jingbo Wang⁴ Yibo Yang⁵
 Yining Li⁴ Kai Chen⁴ Yunhai Tong¹ Bernard Ghanem⁵ Xiangtai Li^{2,4}† Ming-Hsuan Yang^{3,6}
¹ Peking University ² Nanyang Technological University ³ UC, Merced, ⁴ Shanghai AI Laboratory
⁵ KAUST ⁶ Google Research

Project Page: https://xushilin1.github.io/rap_sam/

Abstract

Advanced by transformer architecture, vision foundation models (VFMs) achieve remarkable progress in performance and generalization ability. Segment Anything Model (SAM) is one remarkable model that can achieve generalized segmentation. However, most VFMs cannot run in real-time, which makes it difficult to transfer them into several products. On the other hand, current real-time segmentation mainly has one purpose, such as semantic segmentation on the driving scene. We argue that diverse outputs are needed for real applications. Thus, this work explores a new real-time segmentation setting, named all-purpose segmentation in real-time, to transfer VFMs in real-time deployment. It contains three different tasks, including interactive segmentation, panoptic segmentation, and video segmentation. We aim to use one model to achieve the above tasks in real-time. We first benchmark several strong baselines. Then, we present Real-Time All Purpose SAM (RAP-SAM). It contains an efficient encoder and an efficient decoupled decoder to perform prompt-driven decoding. Moreover, we further explore different training strategies and tuning methods to boost co-training performance further. Our code and model are available at <https://github.com/xushilin1/RAP-SAM/>.

1. Introduction

Recent advancements in computer vision, propelled by transformer architectures [2, 13, 75], focus on developing a singular, large-scale model versatile enough for various tasks, including detection and segmentation, with a general-purpose design. Specifically, several studies [74, 80] adopting identical architectures have demonstrated superior performance compared to models designed exclu-

*The work is done during the internship at Shanghai AI Laboratory. The first two authors share equal technical contributions. † Project Leader.

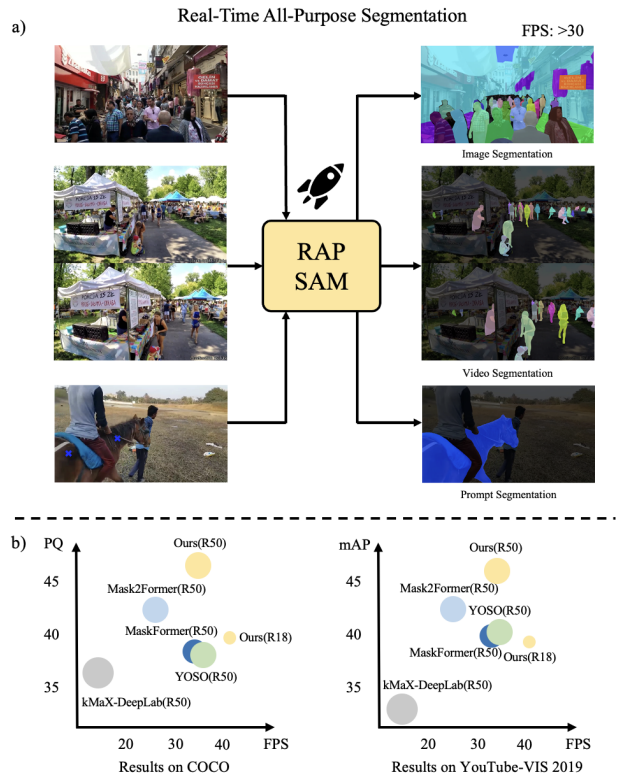


Figure 1. We present real-time all-purpose segmentation to segment and recognize objects for image, video, and interactive inputs. In addition to benchmarking, we also propose a simple yet effective baseline, named RAP-SAM, which achieves the best accuracy and speed trade-off among three different tasks. Both real-time panoptic segmentation and video instance segmentation are shown at the bottom.

sively for specific tasks. Furthermore, numerous studies [30, 34] investigate the foundation model design using extensive data. A notable example, the Segment Anything Model (SAM) [34], introduces an interactive model

driven by visual prompts for versatile segmentation. Concurrently, for semantic-level segmentation, numerous studies [10, 29, 46, 47, 93] employing a universal design have surpassed previous models tailored for specific image and video segmentation tasks.

However, the majority of these studies face challenges in achieving real-time performance or compatibility with mobile devices, primarily due to their *heavy encoders* and *cascaded decoders*. This constraint significantly limits the applicability of these advanced architectures in practical vision applications, although they can achieve high performance. On the contrary, various studies explore real-time segmentation using distinctive designs. Yet, these efforts predominantly concentrate on singular application purposes, including autonomous driving scenes, the COCO dataset for panoptic segmentation (PS) [50], and real-time video instance/object segmentation (VIS) [81]. Currently, no studies investigate real-time, all-purpose segmentation, wherein a model is capable of performing universal segmentation tasks, encompassing image segmentation, video instance/video segmentation, and SAM-like interactive segmentation.

Inspired by the aforementioned challenges, this study investigates the novel issue of real-time, all-purpose segmentation. We pose a critical inquiry: given the limited computational resources and model capacity, how can we develop an efficient, all-purpose segmentation model? This entails creating a single model capable of segmenting, tracking, and classifying each pixel in real-time, akin to performing interactive segmentation similar to SAM.

Initially, we define this research problem by integrating existing benchmarks. Specifically, we use the COCO [50] and YouTube-VIS 2019 [81] datasets for joint co-training, employing identical hyper-parameters. Beyond the semantic queries used for semantic-level segmentation in prior research, our approach additionally incorporates visual prompt queries in SAM for interactive segmentation. However, there are still several challenges: 1), No previous works explore joint co-training for three different purposes. Thus, extensive experiments are needed to search for a better meta-architecture. 2), Interactive segmentation and semantic-level segmentation need better strategies to balance each other. 3), Under the real-time setting, several previous architectures [42, 80] for multi-task segmentation may not be practical.

To address these challenges, we benchmark several recent works [10, 25, 85] in a real-time setting. Then, we initially investigate a range of meta-architectures suitable for all-purpose segmentation. Unlike previous works, we avoid cascaded architecture and only use the pyramid feature once when performing dynamic convolution. We explore four different architectures in the case of various decoder designs, where we adopt a single decoder with multiple

queries. Via extensive experiments, we adopt pooling-based dynamic convolution to replace per-pixel cross-attention to achieve better accuracy and speed trade-off. To balance interactive and semantic-level segmentation, we present an effective dual adapter design that better adapts shared knowledge of the same decoder. Finally, we term our best model as Real-time All-Purpose SAM (RAP-SAM). To the best of our knowledge, it is the first real-time all-purpose segmentation model. Moreover, due to the semantic level and interactive level segmentation ability, our model can also create more new applications, such as interactive video segmentation. Extensive experiments show the effectiveness of our design. The main contributions of this work are:

- We introduce all-purpose segmentation, a multi-task segmentation that aims to segment objects for image, video, and interactive inputs in real-time.
- We benchmark several real-time transformer-based segmentation approaches for the new settings.
- We present a simple yet fast baseline named RAP-SAM. It contains a lightweight feature extractor, a unified decoder, and two asymmetric adapters.
- Extensive experiments demonstrate that RAP-SAM achieves the best speed and accuracy trade-off in the proposed benchmark and regular real-time semantic and panoptic segmentation benchmarks. We also show scalability across datasets and application demos.

2. Related Work

Universal Segmentation. Prior research has focused on designing segmentation models tailored for specific tasks. Recent developments in this field [2, 10, 13, 17, 39, 42, 43, 45, 49, 52, 85–87, 93] have shifted towards employing mask classification architectures, coupled with an end-to-end set prediction objective, to facilitate universal segmentation. This approach has outperformed specialized models [4, 6, 7, 20, 27, 33, 40, 41, 48, 88, 96] across various segmentation tasks, including those involving images, videos, and point clouds [9, 32, 46, 47, 67, 78, 79]. Specifically, Mask2Former [10] uses a masked-attention mechanism and surpasses the performance of prior specific image segmentation models. Similarly, Tube-Link [46] outperforms earlier models [40, 47, 51] tailored for specific video segmentation tasks. Semantic-SAM [35], built on Mask-DINO [36], employs a hybrid query design to facilitate both panoptic and interactive segmentation within a single framework. However, despite the strong performance of these works, their complexity, stemming from the heavier encoder and the cascaded decoder designs, poses significant challenges for integration into actual products. These are primarily hindered by slow processing speeds and substantial parameter overhead.

Vision Foundation Model. Recent advancements in the vision research community have been propelled by the

development of Vision Foundation Models (VFMs), including pure-visual pre-training [19], vision-language pre-training [15, 37], and multi-modal models employing visual prompting [1, 75]. SAM [34] stands as a seminal work targeting general interactive segmentation. Subsequent studies [3, 12, 77] have adapted SAM for diverse applications, predominantly employing it as a segmentation tool. However, these Vision Foundation Models typically employ substantial visual encoders, like ViT-base [13], which poses challenges for deployment on real-time or mobile devices due to their size.

Efficient Model Design. This research direction primarily concentrates on the development of efficient CNNs [18, 23, 24, 28, 56, 66, 94], transformers [57, 58, 64], and hybrid architectures [8, 38, 55, 90, 100], aimed at advancing visual representation learning. Most research investigates backbone design within the constraints of real-time processing and parameter efficiency. These studies are orthogonal to our own, which primarily explores the impact of data, task, and decoder design. Additionally, our work employs efficient models as encoders and presents detailed benchmarks and analyses of the encoder’s effects.

Efficient Segmentation. Previous studies [22, 25, 44, 59, 71, 83, 84, 95] on efficient segmentation have predominantly concentrated on closed-set and specific domains. In particular, a significant portion of this research [25, 44, 60] is dedicated to driving scenarios. Recently, various studies [71, 92, 99] have developed efficient segmentation techniques that facilitate model execution on mobile devices. Mobile SAM [89] introduces a streamlined encoder distillation method. Fast SAM [97] employs a single-stage instance segmentation framework that directly decodes class-agnostic masks. Recently, multiple studies have been conducted on efficient panoptic segmentation [25, 63, 69] and rapid video instance segmentation [82, 91]. However, these real-time segmentation methods are limited to specific tasks. We contend that an all-purpose model capable of real-time performance would have wide-ranging applications in editing, tracking, and segmentation functionalities within various products.

3. Problem Setup

Settings. Our proposed real-time all-purpose segmentation contains three visual inputs, including image, video, and visual prompts (boxes and points). It outputs corresponding masks, labels, and instance ID. We adopt panoptic segmentation for image segmentation, which unifies semantic and instance segmentation. For video segmentation, we adopt video instance segmentation, where we aim to segment and track each foreground instance. For interactive segmentation, we follow the SAM-like setting, where we perform class-agnostic segmentation according to the user’s inputs. Compared with previous settings, as shown in Tab. 1, we

Table 1. Real-Time Segmentation Settings. Our all-purpose segmentation supports more tasks in one framework.

Property	Image Seg	Video Seg	SAM-Like	Ours
Image Masks	✓	✗	✓	✓
Video Masks	✗	✓	✗	✓
Interactive	✗	✗	✓	✓
Semantic Labels	✓	✓	✗	✓
Multi tasks	✗	✗	✗	✓

can achieve more flexible input and output, which is more challenging. Combined with interactive segmentation and video segmentation, we can also achieve interactive video segmentation as video object segmentation.

Datasets. For image segmentation and interactive segmentation, we use the well-known COCO dataset [50] for benchmarking. We adopt partially SAM data [34] for testing. Due to the limited resources and limited model capacity in real-time settings, we do not use SAM data for training. We take COCO data as SAM data for training and testing, where the boxes and random points sampled from masks are used for visual prompting. For video segmentation, we adopt the widely used YouTube-VIS 2019 dataset [81] for training. We *do not* use the SAM data for our benchmarking. There are several reasons: (1), SAM data is not well annotated as the COCO dataset. (2), We only focus on object-level and scene-level segmentation, while SAM data contain more granularity. (3), SAM data has no semantics, while our goal is to predict mask labels for real applications.

4. Proposed Method

Motivation. Employing the same formulation, we first revisit three tasks: panoptic segmentation, video instance segmentation, and interactive segmentation. When combined with a query-based mask transformer, object queries can represent all entities within the scene, encompassing image-level objects, video-level tracked objects, and prompt-based specific objects. Each task’s formulation is as follows:

For panoptic segmentation [33], given an input image $I \in \mathbb{R}^{H \times W \times 3}$, the objective is to generate a group of masks $\{y_i\}_{i=1}^N = \{(m_i, c_i)\}_{i=1}^N$ where c_i denotes the ground truth class label of the binary mask m_i and N is the number of masks, $H \times W$ indicates the spatial dimensions.

For video instance segmentation [81], given a video clip input $V \in \mathbb{R}^{T \times H \times W \times 3}$, where T denotes the number of frames, the process aims to generate an instance mask tube $\{y_i\}_{i=1}^N = \{(m_i, c_i, d_i)\}_{i=1}^N$, where N represents the number of the tube masks $m_i \in \{0, 1\}^{T \times H \times W}$, c_i indicates the class label of the tube m_i , and d_i identifies the instance ID for each tube.

For SAM-like interactive segmentation [34], both the image I and visual prompts $P \in \mathbb{R}^{K \times 4}$ (box prompts are

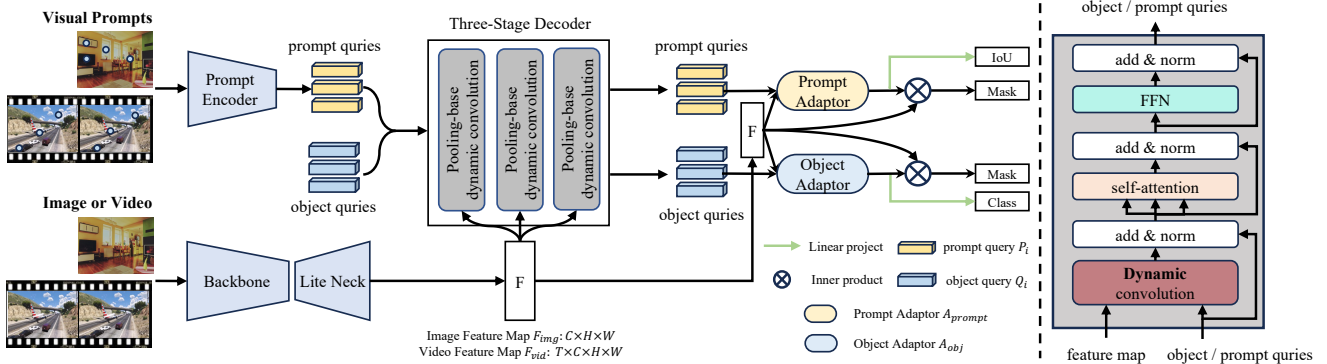


Figure 2. **RAP-SAM overview.** Our method contains three visual inputs: image, video, and visual prompts. Utilizing positional encoding, we generate prompt queries from these visual prompts. The learnable object queries, alongside the prompt queries and the feature map F , are directed to the multi-stage decoder. This process generates multi-stage predictions and refined queries. These refined queries engage in cross-attention with F , resulting in the final prediction.

Table 2. Comparison of Segmentation Methods. Our proposed RAP-SAM supports various segmentation tasks, and it can run in real time.

Methods	SS	PS	VIS	Interactive	Multi-Task in One Model	Real Time
ICNet [95]	✓	✗	✗	✗	✗	✓
Bi-Seg [84]	✓	✗	✗	✗	✗	✓
YOSO [25]	✓	✓	✗	✗	✗	✓
Mobile-VIS [91]	✗	✗	✓	✗	✗	✓
SAM [34]	✗	✗	✗	✓	✗	✗
Mask2Former [10]	✓	✓	✗	✗	✗	✗
Video K-Net [47]	✗	✓	✓	✗	✗	✗
OneFormer [29]	✓	✓	✗	✗	✓	✗
RAP-SAM (Ours)	✓	✓	✓	✓	✓	✓

used here) are taken as inputs. These prompts, which include points and boxes, lead to the outputs of corresponding binary image masks $\{y_i\}_{i=1}^K = \{m_i \in \{0, 1\}^{H \times W}\}_{i=1}^K$, where K denotes the number of visual prompts. Each visual prompt is encoded into one object query, which naturally can be the input of the decoder, as implemented in [10, 34].

Single Object Query For All Segmentation. As mentioned above, by combining all three settings into one, we can represent all the output segmentation entities using the same query-based mask classification framework. In particular, one object query corresponds to one mask m_i , one label c_i , and one ID d_i . We aim to design a simple, efficient, and parameter-sharing framework to support these tasks.

Compared Baselines. In Sec. 5.1, we benchmark several baselines for our all-purpose segmentation. We use the prompt encoder (proposed in SAM [34]) to encode the visual prompt and jointly learn with object query for both PS and VIS on a shared decoder. Although we adopt the lightweight design to speed up, their performance is still limited or not balanced, as shown in Tab 3.

4.1. RAP-SAM Architecture

Overall Architecture. Our RAP-SAM is a simple encoder and decoder architecture. As shown in Fig. 2, it contains a backbone, a lightweight neck, and a shared multitask decoder. Visual prompts P are also the input of the decoder. Following SAM, we also adopt the prompt encoder to encode visual prompts into a query. We adopt the same decoder for both visual prompts and initial object queries to share more computation and parameters. However, the goals of both are different. The former pays more attention to the local details, while the latter also considers the scene and temporal features. To better balance the results for interactive segmentation and image/video segmentation, we design a prompt adaptor and an object adaptor in the end of the decoder.

Lite Feature Extractor. Due to computation cost limitation, we avoid the design of previous methods, such as a large backbone and heavier transformer encoder. We explore lightweight backbones, including ResNet18 [21], STDC-v1 [14], and SeaFormer [71]. We adopt feature pyramid networks with deformable convolutions to fuse multi-scale features and obtain more aligned feature representation, motivated by previous works [44] on real-time semantic segmentation. For video input, we extract the spatial-temporal features. For simplicity, we use $F_{img} \in \mathbb{R}^{\frac{H}{4} \times \frac{W}{4} \times d}$ for image inputs and $F_{vid} \in \mathbb{R}^{T \times \frac{H}{4} \times \frac{W}{4} \times d}$ for video inputs.

Unified Dynamic Convolution Decoder. As in previous works, the goal of the decoder is to refine the object query. However, many of these approaches are impractical for real-time settings due to their reliance on heavily cascaded layers and pixel-wise cross-attention mechanisms. In contrast, our method employs a pooling-based dynamic convolution framework [47, 93] to enhance the decoder’s efficiency.

Given object query $Q_i \in \mathbb{R}^{N \times d}$ and prompt query $P_i \in$

$\mathbb{R}^{K \times d}$, the initial masks M_i are obtained by dot product with F_{img} or F_{vid} . i denotes the index of the decoder stage. According to the inputs, the masks can be image masks for panoptic segmentation $M_i^{pan} \in \mathbb{R}^{N \times \frac{H}{4} \times \frac{W}{4}}$ and interactive segmentation $M_i^{iter} \in \mathbb{R}^{K \times \frac{H}{4} \times \frac{W}{4}}$ or tube masks $M_i^{tube} \in \mathbb{R}^{N \times T \times \frac{H}{4} \times \frac{W}{4}}$. Then, we can obtain the corresponding query features $X_i^{pan} \in \mathbb{R}^{N \times d}$, $X_i^{iter} \in \mathbb{R}^{K \times d}$, $X_i^{tube} \in \mathbb{R}^{N \times d}$ via mask pooling:

$$X_i^{pan} = \sum_u^W \sum_v^H M_{i-1}^{pan}(u, v) \cdot F_{img}(u, v). \quad (1)$$

For video tasks, we group the spatial-temporal features as follows:

$$X_i^{tube} = \sum_t^T \sum_u^W \sum_v^H M_{i-1}^{tube}(t, u, v) \cdot F_{vid}(t, u, v), \quad (2)$$

where u, v are the indices of spatial location, t is index of input frame. Since the dynamic convolution performs similarly for each task, we use panoptic segmentation X_i^{pan} as an illustration. For interactive segmentation, we adopt the same equation (Equ. 1). In our implementation, the learned query is shared for both Q_i^{pan} and Q_i^{tube} .

In particular, we adopt the design [42, 68, 93] to refine input queries Q_i^{pan} with features X_i^{pan} which are grouped from their masks,

$$\hat{Q}_i^{pan} = \text{DynamicConv}(X_i^{pan}, Q_{i-1}^{pan}), \quad (3)$$

where the dynamic convolution uses the query features X_i^{pan} to generate parameters to weight input queries Q_{i-1}^{pan} . Specifically, DynamicConv uses input query features X_i^{pan} to generate gating parameters via a multilayer perceptron (MLP) and multiply back to the original query input Q_{i-1}^{pan} . We adopt the same design [68, 93] by learning gating functions to update the refined queries. The DynamicConv operation is based on:

$$\hat{Q}_i^{pan} = \text{Gate}_x(X_i^{pan})X_i^{pan} + \text{Gate}_q(X_i^{pan})Q_{i-1}^{pan}, \quad (4)$$

where Gate is implemented with a fully connected (FC) layer followed by Layer Norm (LN) and a sigmoid layer. We adopt two different gate functions, including Gate_x and Gate_q . They are implemented by MLP. The former is to weigh the query features, while the latter is to weigh corresponding queries. Next, we adopt one self-attention layer with feed-forward layers [70, 72] to learn the correspondence among each query and update them accordingly. This operation leads to the full correlation among queries, shown as follows:

$$Q_i = \text{FFN}(\text{MHSA}(\hat{Q}_i) + \hat{Q}_i), \quad (5)$$

where MHSA means Multi Head Self Attention, FFN is the Feed Forward Network commonly used in the current version of Transformers [2, 13]. Finally, the refined masks are obtained via dot product between the refined queries Q_i^{pan} , and the input features F_p, F_s . For mask classification, we adopt several feed-forward layers on Q_i^{pan} and directly output the class scores. Then, we perform the inner product between the learned queries Q_i^{pan} , Q_i^{iter} , and their features F_{vid} and F_{img} . For the video segmentation task, the only difference is that we predict the tube mask rather than the image mask. The entire process (Equ. 1, Equ. 2, Equ. 3 and Equ. 5) is repeated three times in total.

Moreover, we also explore various decoupled designs, as shown in Fig. 3. In particular, as previous works suggest, we also explore decoupled decoders and their corresponding adapters. Via our detailed experiments, we do not find extra gains in the cases of decoupled decoders that introduce more computation and parameter costs. Please refer to Sec. 5.2 for the detailed decoder design.

Light-Weight Decoupled Adapter. After the shared decoder, we also add two lightweight adapters, A_{obj} and A_{prompt} to adapt the shared decoder’s knowledge better. In particular, we use the asymmetric design. A_{obj} uses the same dynamic convolution design to refine the object query further, while A_{prompt} uses pixel-wise cross-attention design. Our key insights are: (1) For panoptic segmentation and video segmentation, the interaction of the scene feature is necessary, but not for interactive segmentation. (2) despite the decoder being shared, the details are still missing for interactive segmentation due to the pooling effect in Equ. 1, where we even find inferior results after adopting a pooling-based adapter. More detailed adapter design can be found in Sec. 5.2.

4.2. Training and Inference

Joint Image and Video Segmentation Co-training. Our goal is to train all segmentation tasks only once jointly. All training targets are one entity label and mask for all three different cases. The entity can be thing, stuff, class-agnostic masks, and their corresponding labels. Note that the instance masks with the same ID d form the tube masks. During training, we apply Hungarian matching between the predicted and ground-truth entity masks to assign object queries to video/image entities and then supervise their predicted masks and classification. The classifier is replaced by CLIP text embedding to avoid cross-dataset taxonomy conflicts.

Following previous works [10, 46], the final loss function is given as $L = \lambda_{cls}L_{m_cls} + \lambda_{ce}L_{m_ce} + \lambda_{dice}L_{m_dice}$. Here, L_{m_cls} is the Cross-Entropy (CE) loss for mask classification, and L_{m_ce} and L_{m_dice} are mask Cross-Entropy (CE) loss and Dice loss [62, 73] for segmentation, respectively. By default, we set $\lambda_{cls} = 2, \lambda_{ce} = 5, \lambda_{dice} = 5$.

Table 3. Real-Time All-Purpose Segmentation benchmark. Our proposed RAP-SAM achieves the best accuracy and speed trade-off on three tasks.

Method	Backbone	COCO-Panoptic				COCO-SAM	YouTube-VIS 2019	Flops	Parameters	FPS
		PQ	SQ	PQ _{th}	PQ _{st}	mIoU	mAP			
Mask2Former [10]	R18	35.6	77.5	39.0	30.3	54.7	38.6	89.8G	18.6M	31.2
Mask2Former [10]	R50	42.9	79.8	47.6	35.6	58.0	42.1	153G	45.2M	26.6
MaskFormer [11]	R18	31.0	76.0	33.2	27.7	55.6	34.1	79.7G	18.5M	38.0
MaskFormer [11]	R50	37.4	77.3	41.2	31.8	58.8	40.0	143.0G	45.2M	34.3
MaskFormer [11]	TopFormer [92]	31.6	75.9	33.5	28.6	56.1	38.2	60.0G	12.8M	29.9
kMaX-DeepLab [85]	R18	27.8	71.0	30.3	24.1	16.9	23.1	87.1G	18.7M	15.0
kMaX-DeepLab [85]	R50	36.9	75.7	42.7	28.4	20.1	26.4	280.0G	51.4M	14.9
YOSO [25]	R18	31.6	76.8	36.4	24.4	45.7	31.4	57.3G	18.7M	41.0
YOSO [25]	R50	37.3	76.9	42.7	29.2	49.2	40.7	119.0G	45.1M	36.3
YOSO [25]	TopFormer [92]	31.0	75.9	33.0	26.9	45.1	27.9	36.8G	12.9M	31.1
RAP-SAM	R18	39.9	78.6	43.3	34.8	52.7	38.7	60.5G	22.8M	40.3
RAP-SAM	R50	46.9	80.8	51.6	39.8	57.9	46.2	123.0G	47.2M	35.1
RAP-SAM	TopFormer [92]	34.6	77.0	37.8	29.8	53.3	41.7	40.1G	15.0M	30.7

Inference. we follow the same inference procedure of Mask2Former [10] for image segmentation. We merge the things and stuff for PS according to the sorted scores. The scores are generated by CLIP text embedding. For video instance segmentation, we use query matching rather than introducing extra tracking components to generate instance ID, following previous work [26, 46, 47]. We adopt a near-online method for inference. For interactive segmentation tasks, we follow the origin SAM [34], by providing box and point prompts and obtaining the binary masks. All the parameters are *shared* across three different tasks.

Extension and Application. Since our model can perform various segmentation tasks, RAP-SAM can be extended to more datasets and tasks, including semantic segmentation on ADE20k [98] or video panoptic segmentation on VIPSeg [61]. Moreover, our method can support prompt-driven video object segmentation by combining interactive segmentation with a video instance segmentation framework. We put the details of the extension and application for RAP-SAM in the supplementary.

5. Experiments

Datasets. Our benchmark uses COCO [50] and YouTube-VIS 2019 [81] datasets for benchmarking. COCO-SAM is constructed by using ground truth boxes and masks as visual prompt inputs, following the SAM-1B dataset [34]. In addition, to verify the effectiveness and generality of RAP-SAM, we also use other datasets, including ADE-20K [98] and VIP-Seg dataset [61] in Sec. 5.1.

Evaluation Metrics and Devices. For image segmentation, we adopt panoptic quality (PQ), which can be further decomposed into the segmentation quality (SQ) and the recognition quality (RQ). For the VIS task, mAP is adopted. We further report the semantic segmentation results (mIoU) and video panoptic segmentation results (STQ [76] and VPQ [31]). We adopt one A100 GPU for speed testing.

Re-implemented Baselines. Since no previous works explore joint co-training for image, video, and interactive segmentation in one framework. We re-implement several representative baselines using the same codebase, including non-real-time models (Mask2Former [10], kMaX-DeepLab [85]) for reference. In particular, we benchmark over ten different methods, including different backbones and decoders.

Implementation Details. We implement our models and all other baselines in PyTorch [65] with the MMDetection toolbox [5]. We use the distributed training framework with 16 A100 GPUs. Each mini-batch has two images per GPU. In particular, we adopt pseudo video training on COCO by moving image masks with random directions. All the models are trained with 24 epochs. For data augmentation, we adopt large-scale jitter as previous works [10] to build strong baselines. For all models, we adopt training steps and optimizers. Refer to the supplementary for more details.

5.1. Main Results

Our Benchmark Results. We list our benchmark results in Tab. 3. We benchmark recent state-of-the-art methods using the same training and test settings. From the table, our proposed RAP-SAM achieves the best speed and accuracy trade-off on all three different visual segmentation tasks, under the various backbones. Mask2Former [10] achieves similar or partially stronger results than our method. However, their speed is still limited, which is 7-8 FPS slower than our methods. YOSO [25] runs as fast as our method. However, the performance gap is still significant. Thus, our proposed RAP-SAM is a simple yet effective baseline for real-time and all-purpose settings.

Promptable Results Compared with SAM. In Tab. 4, we verify our trained model as a promptable segmenter, like SAM. We compare our method with SAM-Huge, which is

Table 4. Comparison with SAM [34] as a promptable segmenter on various detectors and instance segmenters.

Method	Detectors	mAP	AP50	AP75	Parameters	Flops
SAM-Huge	Mask-RCNN (R50)	35.6	54.9	38.4	641M	3000G
Ours	Mask-RCNN (R50)	26.7	43.0	27.9	47M	188G
SAM-Huge	Mask-RCNN (X-101-64x4d)	39.0	60.5	42.1	641M	3000G
Ours	Mask-RCNN (X-101-64x4d)	28.5	46.4	29.9	47M	188G

Table 5. Comparison with real-time video segmentation method on VIP-Seg validation set.

Method	backbone	VPQ ¹	VPQ ²	VPQ ⁴	VPQ ⁶	VPQ	STQ	FPS
Clip-PanoFCN [61]	R50	24.3	23.5	22.4	21.6	22.9	31.5	8
Video K-Net [47]	R50	29.5	26.5	24.5	23.7	26.1	33.1	10
Tube-Link [46]	STDCv1	32.1	31.3	30.1	29.1	30.6	32.0	14
Tube-Link [46]	STDCv2	33.2	31.8	30.6	29.6	31.4	32.8	12
Ours	R18	34.2	32.1	30.8	30.2	32.5	33.7	30

Table 6. Comparison with real-time panoptic segmentation method on ADE-20k validation set.

Method	Backbone	PQ	PQ th	PQ st	Parameters	Flops
PanSegFormer [49]	R50	36.4	35.3	38.6	51M	214G
MaskFormer [11]	R50	34.7	32.2	39.7	45.2M	181G
Mask2Former [10]	R50	39.7	39.0	40.9	45.2M	226G
YOSO [25]	R50	38.0	37.3	39.4	45.1M	176G
RAP-SAM	R50	38.3	36.6	39.7	47.2M	179G

much larger. Despite there being a gap, our method can run fast and with much less GFlops.

Comparison with Specific Design Models on VIP-Seg. We also verify the effectiveness of RAP-SAM on a more challenging video segmentation task, video panoptic segmentation on the VIP-Seg dataset. Compared with recent works [46, 61], RAP-SAM also archives the best speed and accuracy trade-off.

Comparison with Specific Design Models on ADE-20k. We further transfer RAP-SAM on ADE-20k datasets. Since our method is real-time model, we only list several representative works for reference. Again, compared with recent work [25], our method still achieves stronger results.

5.2. Ablation Study and Visual Analysis

Ablation on Shared Decoder Design. In Tab. 7, we find using simple pooling-based dynamic convolution performs well under real-time settings, where we adopt R18 as the backbone and keep the adapter unchanged. In particular, there is no difference in panoptic segmentation results and a slight gap for interactive segmentation. However, per-pixel cross-attention introduces extra computation costs.

Ablation on Meta-Architecture Design. In Tab. 8, we further explore the meta-architecture design, as shown in Fig. 3. We use R50 as the backbone and keep the adapter unchanged. From the table, we find using a shared decoder architecture (in Tab. 7) achieves the best parameter and performance trade-off. These findings may conflict with recent multi-task works [42] since the decoupled decoders may

Table 7. Ablation on shared decoder design.

Setting	COCO-Panoptic	COCO-SAM	FPS
Per-Pixel Cross-Attention [10]	45.0	55.3	28.0
Pooling + Dynamic Convolution [68]	43.8	55.7	36.2
Pooling + Dynamic Convolution with Gate [93]	44.6	56.7	34.5

Table 8. Ablation on meta-architecture.

Setting	COCO-Panoptic	COCO-SAM	Parameters
Fig. 3 (a)	43.8	54.2	46.3M
Fig. 3 (b)	44.0	55.2	53.6M
Fig. 3 (c)	44.6	56.7	47.3M
Fig. 3 (d)	45.2	56.2	54.6M

Table 9. Ablation on adapter design. CA: cross-attention. DC: dynamic convolution.

A _{obj}	A _{prompt}	COCO-Panoptic	COCO-SAM
-	-	44.2	53.2
CA	CA	42.6	54.3
DC	DC	44.7	52.1
DC	CA	44.6	56.7
CA	DC	44.5	56.2

Table 10. Ablation on joint co-training. (a), COCO-Panoptic. (b), YT-VIS 2019. (c), COCO-SAM.

Setting	COCO-Panoptic	YT-VIS 2019	COCO-SAM
a	36.6	-	-
b	-	21.5	-
a + b	36.2	36.0	50.7
a + b + c	35.7	35.3	50.9

have more capacity. We argue that since our feature extractors are weaker than those works and the representation power is far from the heavier backbone such as Swin [52] or ViT-large [13], adding more capacity in the decoder may not boost the final performance.

Ablation on Adapter Design. Then, we explore the adapter design in Tab. 9. In particular, we use a pre-trained model without adapters for initialization to see the effect of different adapters. In particular, we find using asymmetric adapters works well for balanced results for object queries and prompt queries, since the goals of the two queries are different. The former needs the spatio-temporal and scene-level context, while the latter only cares about the region context with the input position as the guidance.

Effectiveness of Joint Co-training. We further explore the effect of each dataset in Tab. 10. We find joint co-training with image and video data leads to better performance for video instance segmentation. Adding COCO-SAM training leads to a few performance drops. This is because the learning targets are different for object queries and prompt queries.

Visualization. In Fig. 4, we give the three different visualization results on the YouTube-VIS 2019 dataset and

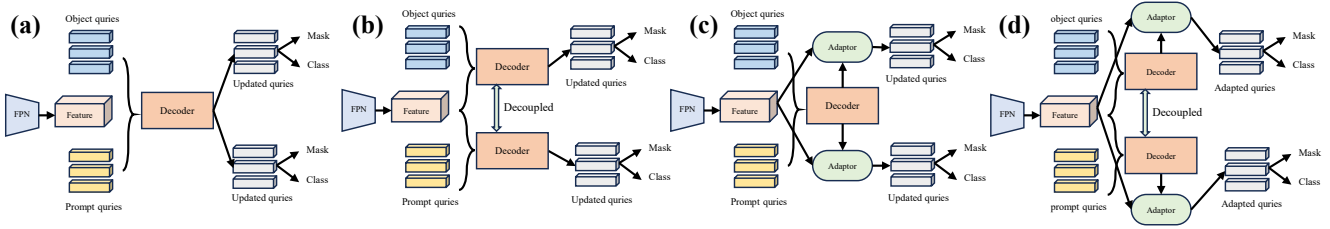


Figure 3. Meta-architecture exploration. (a), Simple shared decoder design. (b), Decoupled decoder design with two heads. (c), Shared decoder with decoupled adapter. (d), Decoupled decoder with the decoupled adapters. Best viewed in color and zoom in.

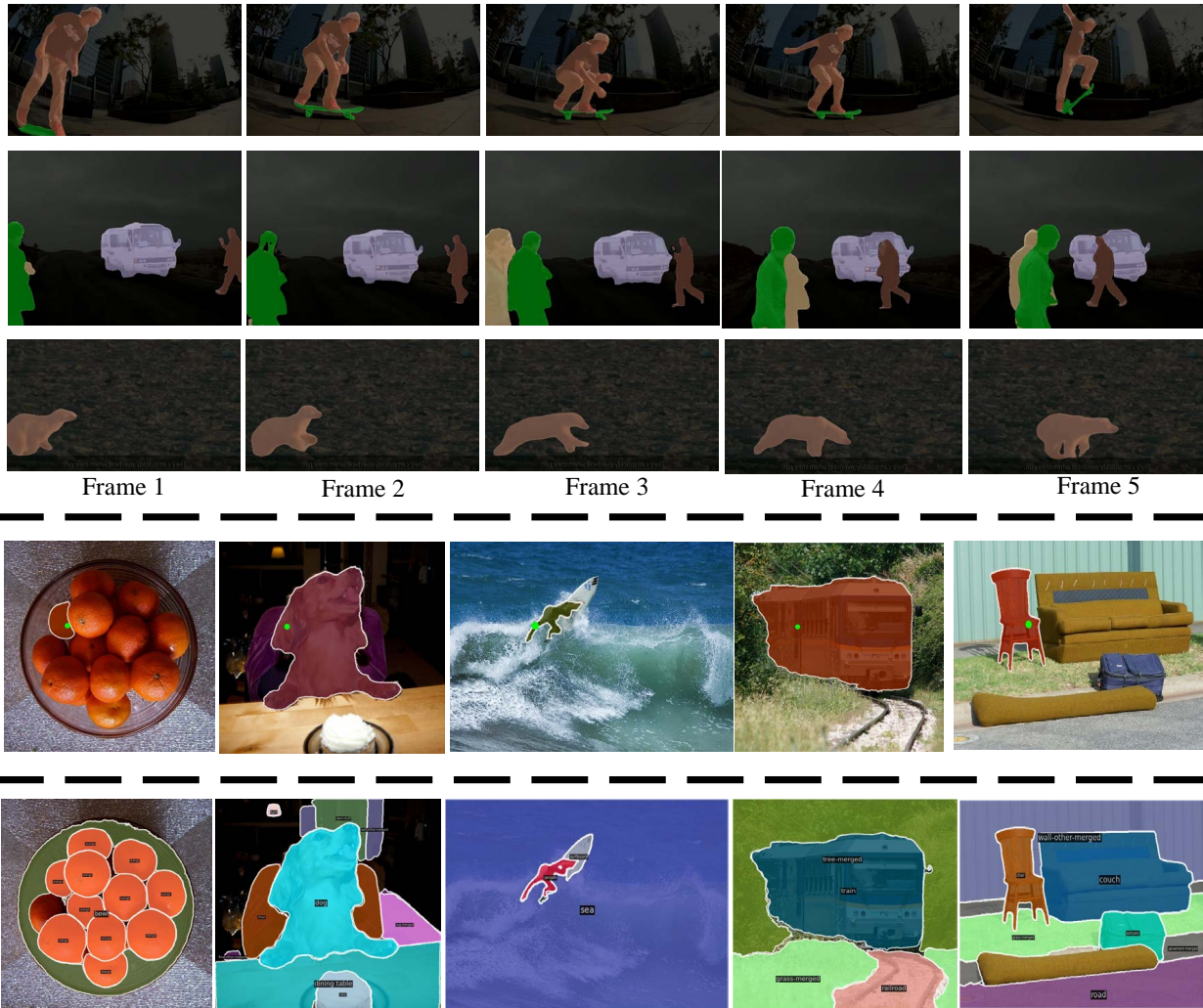


Figure 4. The visualization results of our model on the YouTube-VIS 2019 dataset and the COCO dataset. The first three rows visualize five frames of inputs. The same instances are shown with the same color. The fourth row shows the interactive segmentation results with a single-point prompt (shown in green color). The last row shows the panoptic segmentation results.

the COCO dataset. We generate these visualization results using only a single model thanks to the joint co-training strategy. The first three rows in Fig. 4 show the video instance segmentation. The fourth row shows the interactive

segmentation results with a single-point prompt (shown in green color), and the last row shows the panoptic results.

6. Conclusion

In this work, we explore a challenging real-time setting, all-purpose segmentation, to transfer more segmentation tasks into one model. To solve this problem, we introduce RAP-SAM, a real-time segmentation model, that can segment and track objects in image, video, and interactive modes. We design a simple shared decoder with two key designs: shared dynamic convolution and asymmetric adapters, which lead to the best trade-off between speed and accuracy on three segmentation tasks. We hope our proposed benchmark inspires future research on this new setting.

Overview. In this supplementary, we first present more detailed results to support both the benchmark and our proposed RAP-SAM in Sec. A. Then, in Sec. B, we present a more detailed visual comparison using our model. Finally, in Sec. C, we discuss several failure cases and potential future work.

A. More Experiment Results

Benchmark More Methods. In Tab. 11, we benchmark more models and backbones [57, 58, 93] as the supplementary to main paper. Again, for various backbones and different heads, our model can achieve better or comparable results across three different tasks, while running in real-time. In particular, compared with the dynamic kernel-based method, K-Net, our approach achieves better performance on the R18 and R50 backbones and comparable results on the lightweight backbones.

Scale Up Joint Co-training. In the bottom of Tab. 11, we further scale up our model on a large backbone, ConvNeXt large [53]. From the table, we find there are significant gains in all settings while still running with 8 FPS. This means our proposed all-purposed segmentation still has room to balance the accuracy and inference speed.

Explore adapter Design on More Methods. We explore the effectiveness of our adapter design on Mask2Former [10] and add the adapter module to the last decoder layer of Mask2Former. As shown in Tab. 12, Mask2Former with adapter will improve 1.1 mIoU score compared with origin Mask2Former for interactive segmentation and only drop 0.3 PQ for panoptic segmentation. This result indicates that the adapter module not only applies to our method but can also be generalized to other methods

More Implementation Details. We implement our proposed method and benchmark methods using MMDetection toolbox [5], and we train all of these methods in the same environment. For kMaX-DeepLab [85], we excluded the auxiliary semantic segmentation loss, instance discrimination loss, and preserving PQ-style loss alignment with Mask2former [10] for a fair comparison. We utilize the AdamW [54] optimizer with a weight decay of 0.05, and

the learning rate is set to $1e-4$ for all methods. We warm up the learning rate in the first 500 iterations using a linearly increased strategy and decay the learning rate at 8 and 11 epochs by a factor of 10. For data augmentation, we use the large-scale jittering (LSJ) augmentation [16] with a random scale sampled from the range of 0.1 to 2.0 and followed by a fixed size crop to 1024×1024 .

More Inference Details. For video instance segmentation, we adopt simple object query matching [26, 47] for all methods to keep the fair comparison. For interactive segmentation, we mainly use point prompts, which is more challenging than box prompts. For panoptic segmentation, all hyperparameters are the same. The FPS is obtained on one A100 card for both the main paper and supplementary.

B. Visual Comparison

Comparison on Youtube-VIS dataset. In Fig. 5, we compare our RAP-SAM (right) with a strong baseline Mask2Former (left) with the same ResNet50 backbone. Our methods achieve more consistent tracking and segmentation results in these examples.

Comparison on COCO Panoptic Segmentation dataset. In Fig. 6, We demonstrate that our RAP-SAM model surpasses K-Net in panoptic segmentation tasks. RAP-SAM exhibits enhanced accuracy in processing complex scenes and maintaining fine details, especially in segmenting object edges and managing overlapping objects.

More Interactive Segmentation Results. In Fig. 7, We present further visualizations of interactive segmentation, showcasing segmentation outcomes for 'things' and 'stuff'. In these visualizations, green dots signify manually specified prompts. Our model exhibits precise segmentation abilities for 'things' and 'stuff'. Notably, even when prompt points are situated on object boundaries, our model accurately identifies and segments the object.

C. Challenges and Future Work

Failure Cases Analysis. We also analyze failure cases in video/image segmentation and identify two typical failure modes of RAP-SAM. Firstly, as illustrated in Fig. 8, when faced with multiple objects with high overlap, RAP-SAM struggles to fully recognize them, resulting in the omission of several masks. Secondly, in crowded scenarios, RAP-SAM faces challenges in recognizing and segmenting all instances with a limited number of instance kernels.

Future Work Discussion. There are several directions to explore for real-time all-purpose segmentation. The first direction is to achieve better-balanced performance on image, video, and interactive segmentation (since there is still a lot of room for performance, as shown in the last row of Tab. 11). The second direction is to speed up the model and deploy the model on the edge device, such as iPhone. The

Table 11. Benchmark More Models on Real-Time All-Purpose Segmentation. The GFlops are obtained with 1333×800 inputs.

Method	Backbone	COCO-Panoptic				COCO-SAM	YouTube-VIS 2019	Flops	Parameters	FPS
		PQ	SQ	PQ _{th}	PQ _{st}	mIoU	mAP			
YOSO [25]	EdgeNexT [57]	31.8	74.5	35.6	26.1	47.4	35.4	40G	15.3M	28.6
K-Net [93]	R18 [21]	33.1	75.7	36.8	27.4	53.6	34.8	124G	25.6M	30.4
K-Net [93]	R50 [21]	39.2	78.2	43.9	31.6	56.3	41.7	171G	38.5M	20.9
K-Net [93]	EdgeNexT [57]	38.0	76.7	42.5	31.4	55.7	44.0	108G	19.5M	30.5
Mask2Former [10]	EdgeNexT [57]	39.8	78.8	43.6	34.0	54.2	-	73G	12.0M	25.6
RAP-SAM	R18	39.9	78.6	43.3	34.8	52.7	38.7	60.5G	22.8M	40.3
RAP-SAM	R50	46.9	80.8	51.6	39.8	57.9	46.2	123.0G	47.2M	35.1
RAP-SAM	EdgeNexT [57]	38.0	77.7	42.1	31.9	54.8	46.3	44G	14.3M	31.5
RAP-SAM	ConvNeXt-L [53]	52.3	82.5	58.6	42.8	61.1	55.6	700G	239M	8.6



Figure 5. When compared to the Mask2Former(right) on the YouTube-VIS 2019 dataset, our RAP-SAM(left) demonstrates superior performance in recognizing and segmenting objects in certain scenarios, and it also holds an advantage in detailing edges.

Table 12. Explore adapter Design on More Methods.

Method	Backbone	PQ	mIoU
Mask2Former	R50	43.2	57.0
Mask2Former+adapter	R50	43.0	58.1

third direction is to explore different knowledge distillation approaches to transfer the vision foundation model in real-time all-purpose models. Moreover, more visual prompts can be explored, such as mask prompts or box prompts. Our method currently only supports point prompts. This will be our future work.

References

- [1] Jean-Baptiste Alayrac, Jeff Donahue, Pauline Luc, Antoine Miech, Iain Barr, Yana Hasson, Karel Lenc, Arthur Mensch, Katherine Millican, Malcolm Reynolds, et al. Flamingo: a visual language model for few-shot learning. *NeurIPS*, 2022. 3
- [2] Nicolas Carion, Francisco Massa, Gabriel Synnaeve, Nicolas Usunier, Alexander Kirillov, and Sergey Zagoruyko. End-to-end object detection with transformers. In *ECCV*, 2020. 1, 2, 5
- [3] Cheng Chen, Juzheng Miao, Dufan Wu, Zhiling Yan, Sekeun Kim, Jiang Hu, Aoxiao Zhong, Zhengliang Liu, Lichao Sun, Xiang Li, Tianming Liu, Pheng-Ann Heng, and Quanzheng Li. Ma-sam: Modality-agnostic sam adaptation for 3d medical image segmentation. *arXiv preprint arXiv:2309.08842*, 2023. 3
- [4] Kai Chen, Jiangmiao Pang, Jiaqi Wang, Yu Xiong, Xiaoxiao Li, Shuyang Sun, Wansen Feng, Ziwei Liu, Jianping Shi, Wanli Ouyang, Chen Change Loy, and Dahua Lin. Hybrid task cascade for instance segmentation. In *CVPR*, 2019. 2
- [5] Kai Chen, Jiaqi Wang, Jiangmiao Pang, Yuhang Cao, Yu Xiong, Xiaoxiao Li, Shuyang Sun, Wansen Feng, Ziwei Liu, Jiarui Xu, et al. Mmdetection: Open mmlab detection toolbox and benchmark. *arXiv preprint*, 2019. 6, 9
- [6] Liang-Chieh Chen, George Papandreou, Florian Schroff, and Hartwig Adam. Rethinking atrous convolution for semantic image segmentation. *arXiv:1706.05587*, 2017. 2
- [7] Liang-Chieh Chen, Yukun Zhu, George Papandreou, Florian Schroff, and Hartwig Adam. Encoder-decoder with atrous separable convolution for semantic image segmentation. In *ECCV*, 2018. 2
- [8] Yinpeng Chen, Xiyang Dai, Dongdong Chen, Mengchen Liu, Xiaoyi Dong, Lu Yuan, and Zicheng Liu. Mobile-



Figure 6. When compared with K-Net (bottom) on the COCO dataset, our RAP-SAM (top) model shows a significant advantage, achieving more accurate segmentation of foreground and background, with edges that are smoother.

- former: Bridging mobilenet and transformer. In *CVPR*, 2022. 3
- [9] Bowen Cheng, Anwesa Choudhuri, Ishan Misra, Alexander Kirillov, Rohit Girdhar, and Alexander G Schwing. Mask2former for video instance segmentation. *arXiv preprint*, 2021. 2
- [10] Bowen Cheng, Ishan Misra, Alexander G. Schwing, Alexander Kirillov, and Rohit Girdhar. Masked-attention mask transformer for universal image segmentation. In *CVPR*, 2022. 2, 4, 5, 6, 7, 9, 10
- [11] Bowen Cheng, Alexander G. Schwing, and Alexander Kirillov. Per-pixel classification is not all you need for semantic segmentation. In *NeurIPS*, 2021. 6, 7
- [12] Yangming Cheng, Liulei Li, Yuanyou Xu, Xiaodi Li, Zongxin Yang, Wenguan Wang, and Yi Yang. Segment and track anything. *arXiv preprint arXiv:2305.06558*, 2023. 3
- [13] Alexey Dosovitskiy, Lucas Beyer, Alexander Kolesnikov, Dirk Weissenborn, Xiaohua Zhai, Thomas Unterthiner, Mostafa Dehghani, Matthias Minderer, Georg Heigold, Sylvain Gelly, et al. An image is worth 16x16 words: Transformers for image recognition at scale. *arXiv preprint arXiv:2010.11929*, 2020. 1, 2, 3, 5, 7
- [14] Mingyuan Fan, Shenqi Lai, Junshi Huang, Xiaoming Wei, Zhenhua Chai, Junfeng Luo, and Xiaolin Wei. Rethinking bisenet for real-time semantic segmentation. In *CVPR*, 2021. 4
- [15] Yuxin Fang, Wen Wang, Binhui Xie, Quan Sun, Ledell Wu, Xinggang Wang, Tiejun Huang, Xinlong Wang, and Yue

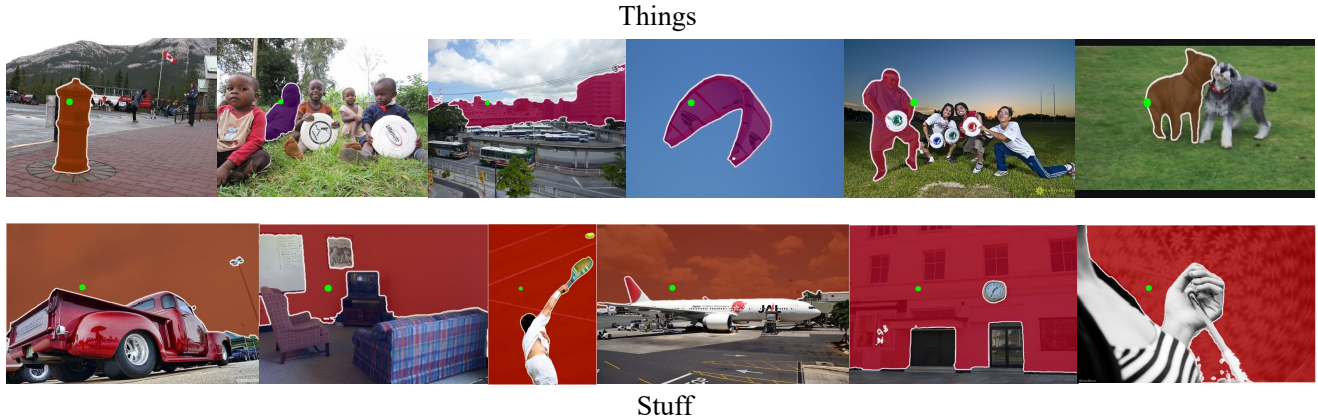


Figure 7. Here are additional results of interactive segmentation. For point prompts or box prompts, RAP-SAM segments out the corresponding object based on the spatial location of the prompt. We have provided both segmentation results for ‘things’ and ‘stuff’, demonstrating that RAP-SAM is capable of segmenting both while maintaining strong performance.



Figure 8. Failure modes of RAP-SAM in image/video segmentation.

- Cao, Eva: Exploring the limits of masked visual representation learning at scale. *arXiv preprint arXiv:2211.07636*, 2022. 3
- [16] Golnaz Ghiasi, Yin Cui, A. Srinivas, Rui Qian, Tsung-Yi Lin, Ekin Dogus Cubuk, Quoc V. Le, and Barret Zoph. Simple copy-paste is a strong data augmentation method for instance segmentation. *CVPR*, 2020. 9
- [17] Xiuye Gu, Yin Cui, Jonathan Huang, Abdullah Rashwan, Xuan Yang, Xingyi Zhou, Golnaz Ghiasi, Weicheng Kuo, Huizhong Chen, Liang-Chieh Chen, et al. Dataseg: Taming a universal multi-dataset multi-task segmentation model. *arXiv preprint arXiv:2306.01736*, 2023. 2
- [18] Kai Han, Yunhe Wang, Qi Tian, Jianyuan Guo, Chunjing Xu, and Chang Xu. Ghostnet: More features from cheap operations. In *CVPR*, 2020. 3
- [19] Kaiming He, Xinlei Chen, Saining Xie, Yanghao Li, Piotr Dollár, and Ross Girshick. Masked autoencoders are scalable vision learners. *CVPR*, 2022. 3
- [20] Kaiming He, Georgia Gkioxari, Piotr Dollár, and Ross Girshick. Mask r-cnn. In *ICCV*, 2017. 2
- [21] Kaiming He, Xiangyu Zhang, Shaoqing Ren, and Jian Sun. Deep residual learning for image recognition. In *CVPR*, 2016. 4, 10
- [22] Weixiang Hong, Qingpei Guo, Wei Zhang, Jingdong Chen, and Wei Chu. Lpsnet: A lightweight solution for fast panoptic segmentation. In *CVPR*, 2021. 3
- [23] Andrew Howard, Mark Sandler, Grace Chu, Liang-Chieh Chen, Bo Chen, Mingxing Tan, Weijun Wang, Yukun Zhu, Ruoming Pang, Vijay Vasudevan, et al. Searching for mobilenetv3. In *ICCV*, 2019. 3
- [24] Andrew G Howard, Menglong Zhu, Bo Chen, Dmitry Kalenichenko, Weijun Wang, Tobias Weyand, Marco Andreetto, and Hartwig Adam. Mobilenets: Efficient convolutional neural networks for mobile vision applications. *arXiv preprint arXiv:1704.04861*, 2017. 3
- [25] Jie Hu, Linyan Huang, Tianhe Ren, Shengchuan Zhang, Rongrong Ji, and Liujuan Cao. You only segment once: Towards real-time panoptic segmentation. In *CVPR*, 2023. 2, 3, 4, 6, 7, 10
- [26] De-An Huang, Zhiding Yu, and Anima Anandkumar. Minvis: A minimal video instance segmentation framework without video-based training. In *NeurIPS*, 2022. 6, 9

- [27] Zilong Huang, Xinggang Wang, Lichao Huang, Chang Huang, Yunchao Wei, and Wenyu Liu. Ccnet: Criss-cross attention for semantic segmentation. In *ICCV*, 2019. 2
- [28] Forrest N Iandola, Song Han, Matthew W Moskewicz, Khalid Ashraf, William J Dally, and Kurt Keutzer. Squeezenet: Alexnet-level accuracy with 50x fewer parameters and 0.5 mb model size. *arXiv preprint arXiv:1602.07360*, 2016. 3
- [29] Jitesh Jain, Jiachen Li, MangTik Chiu, Ali Hassani, Nikita Orlov, and Humphrey Shi. OneFormer: One Transformer to Rule Universal Image Segmentation. *CVPR*, 2023. 2, 4
- [30] Chao Jia, Yinfei Yang, Ye Xia, Yi-Ting Chen, Zarana Parekh, Hieu Pham, Quoc Le, Yun-Hsuan Sung, Zhen Li, and Tom Duerig. Scaling up visual and vision-language representation learning with noisy text supervision. In *ICML*, 2021. 1
- [31] Dahun Kim, Sanghyun Woo, Joon-Young Lee, and In So Kweon. Video panoptic segmentation. In *CVPR*, 2020. 6
- [32] Dahun Kim, Jun Xie, Huiyu Wang, Siyuan Qiao, Qihang Yu, Hong-Seok Kim, Hartwig Adam, In So Kweon, and Liang-Chieh Chen. Tubeformer-deeplab: Video mask transformer. In *CVPR*, 2022. 2
- [33] Alexander Kirillov, Kaiming He, Ross Girshick, Carsten Rother, and Piotr Dollár. Panoptic segmentation. In *CVPR*, 2019. 2, 3
- [34] Alexander Kirillov, Eric Mintun, Nikhila Ravi, Hanzi Mao, Chloe Rolland, Laura Gustafson, Tete Xiao, Spencer Whitehead, Alexander C Berg, Wan-Yen Lo, et al. Segment anything. *ICCV*, 2023. 1, 3, 4, 6, 7
- [35] Feng Li, Hao Zhang, Peize Sun, Xueyan Zou, Shilong Liu, Jianwei Yang, Chunyuan Li, Lei Zhang, and Jianfeng Gao. Semantic-sam: Segment and recognize anything at any granularity. *arXiv preprint arXiv:2307.04767*, 2023. 2
- [36] Feng Li, Hao Zhang, Huaizhe xu, Shilong Liu, Lei Zhang, Lionel M. Ni, and Heung-Yeung Shum. Mask DINO: Towards a unified transformer-based framework for object detection and segmentation. In *CVPR*, 2023. 2
- [37] Junnan Li, Dongxu Li, Caiming Xiong, and Steven Hoi. Blip: Bootstrapping language-image pre-training for unified vision-language understanding and generation. In *ICML*, 2022. 3
- [38] Jiashi Li, Xin Xia, Wei Li, Huixia Li, Xing Wang, Xuefeng Xiao, Rui Wang, Min Zheng, and Xin Pan. Nextvit: Next generation vision transformer for efficient deployment in realistic industrial scenarios. *arXiv preprint arXiv:2207.05501*, 2022. 3
- [39] Xiangtai Li, Henghui Ding, Wenwei Zhang, Haobo Yuan, Guangliang Cheng, Pang Jiangmiao, Kai Chen, Ziwei Liu, and Chen Change Loy. Transformer-based visual segmentation: A survey. *arXiv pre-print*, 2023. 2
- [40] Xiangtai Li, Hao He, Yibo Yang, Henghui Ding, Kuiyuan Yang, Guangliang Cheng, Yunhai Tong, and Dacheng Tao. Improving video instance segmentation via temporal pyramid routing. *T-PAMI*, 2022. 2
- [41] Xiangtai Li, Zhao Houlong, Han Lei, Tong Yunhai, and Yang Kuiyuan. Gff: Gated fully fusion for semantic segmentation. In *AAAI*, 2020. 2
- [42] Xiangtai Li, Shilin Xu, Yibo Yang, Guangliang Cheng, Yunhai Tong, and Dacheng Tao. Panoptic-partformer: Learning a unified model for panoptic part segmentation. In *ECCV*, 2022. 2, 5, 7
- [43] Xiangtai Li, Shilin Xu, Yibo Yang, Haobo Yuan, Guangliang Cheng, Yunhai Tong, Zhouchen Lin, Ming-Hsuan Yang, and Dacheng Tao. Panopticpartformer++: A unified and decoupled view for panoptic part segmentation. *arXiv preprint arXiv:2301.00954*, 2023. 2
- [44] Xiangtai Li, Ansheng You, Zeping Zhu, Houlong Zhao, Maoke Yang, Kuiyuan Yang, and Yunhai Tong. Semantic flow for fast and accurate scene parsing. In *ECCV*, 2020. 3, 4
- [45] Xiangtai Li, Haobo Yuan, Wei Li, Henghui Ding, Size Wu, Wenwei Zhang, Yining Li, Kai Chen, and Chen Change Loy. Omg-seg: Is one model good enough for all segmentation? *arXiv*, 2024. 2
- [46] Xiangtai Li, Haobo Yuan, Wenwei Zhang, Guangliang Cheng, Jiangmiao Pang, and Chen Change Loy. Tube-link: A flexible cross tube baseline for universal video segmentation. In *ICCV*, 2023. 2, 5, 6, 7
- [47] Xiangtai Li, Wenwei Zhang, Jiangmiao Pang, Kai Chen, Guangliang Cheng, Yunhai Tong, and Chen Change Loy. Video k-net: A simple, strong, and unified baseline for video segmentation. In *CVPR*, 2022. 2, 4, 6, 7, 9
- [48] Yanwei Li, Hengshuang Zhao, Xiaojuan Qi, Liwei Wang, Zeming Li, Jian Sun, and Jiaya Jia. Fully convolutional networks for panoptic segmentation. *CVPR*, 2021. 2
- [49] Zhiqi Li, Wenhai Wang, Enze Xie, Zhiding Yu, Anima Anandkumar, Jose M. Alvarez, Tong Lu, and Ping Luo. Panoptic segformer: Delving deeper into panoptic segmentation with transformers, 2021. 2, 7
- [50] Tsung-Yi Lin, Michael Maire, Serge Belongie, James Hays, Pietro Perona, Deva Ramanan, Piotr Dollár, and C Lawrence Zitnick. Microsoft coco: Common objects in context. In *ECCV*, 2014. 2, 3, 6
- [51] Haotian Liu, Rafael A. Rivera Soto, Fanyi Xiao, and Yong Jae Lee. Yolactedge: Real-time instance segmentation on the edge (jetson agx xavier: 30 fps, rtx 2080 ti: 170 fps). *arXiv preprint arXiv:2012.12259*, 2020. 2
- [52] Ze Liu, Yutong Lin, Yue Cao, Han Hu, Yixuan Wei, Zheng Zhang, Stephen Lin, and Baining Guo. Swin transformer: Hierarchical vision transformer using shifted windows. *ICCV*, 2021. 2, 7
- [53] Zhuang Liu, Hanzi Mao, Chao-Yuan Wu, Christoph Feichtenhofer, Trevor Darrell, and Saining Xie. A convnet for the 2020s. *CVPR*, 2022. 9, 10
- [54] Ilya Loshchilov and Frank Hutter. Decoupled weight decay regularization. *arXiv preprint*, 2017. 9
- [55] Hailong Ma, Xin Xia, Xing Wang, Xuefeng Xiao, Jiashi Li, and Min Zheng. MocoVIT: Mobile convolutional vision transformer. *arXiv preprint arXiv:2205.12635*, 2022. 3
- [56] Ningning Ma, Xiangyu Zhang, Hai-Tao Zheng, and Jian Sun. Shufflenet v2: Practical guidelines for efficient cnn architecture design. In *ECCV*, 2018. 3
- [57] Muhammad Maaz, Abdelrahman Shaker, Hisham Cholakkal, Salman Khan, Syed Waqas Zamir, Rao Muhammad Anwer, and Fahad Shahbaz Khan. Edgenext: efficiently amalgamated cnn-transformer architecture for mobile vision applications. 2022. 3, 9, 10
- [58] Sachin Mehta and Mohammad Rastegari. Mobilevit: Light-

- weight, general-purpose, and mobile-friendly vision transformer. In *ICLR*, 2022. 3, 9
- [59] Sachin Mehta, Mohammad Rastegari, Anat Caspi, Linda Shapiro, and Hannaneh Hajishirzi. Espnet: Efficient spatial pyramid of dilated convolutions for semantic segmentation. In *ECCV*, 2018. 3
- [60] Sachin Mehta, Mohammad Rastegari, Linda Shapiro, and Hannaneh Hajishirzi. Espnetv2: A light-weight, power efficient, and general purpose convolutional neural network. In *CVPR*, 2019. 3
- [61] Jiayu Miao, Xiaohan Wang, Yu Wu, Wei Li, Xu Zhang, Yunchao Wei, and Yi Yang. Large-scale video panoptic segmentation in the wild: A benchmark. In *CVPR*, 2022. 6, 7
- [62] Fausto Milletari, Nassir Navab, and Seyed-Ahmad Ahmadi. V-Net: Fully convolutional neural networks for volumetric medical image segmentation. In *3DV*, 2016. 5
- [63] Rohit Mohan and Abhinav Valada. Efficientps: Efficient panoptic segmentation. *IJCV*, 2021. 3
- [64] Junting Pan, Adrian Bulat, Fuwen Tan, Xiatian Zhu, Lukasz Dudziak, Hongsheng Li, Georgios Tzimiropoulos, and Brais Martinez. Edgevids: Competing light-weight cnns on mobile devices with vision transformers. *ECCV*, 2022. 3
- [65] Adam Paszke, Sam Gross, Francisco Massa, Adam Lerer, James Bradbury, Gregory Chanan, Trevor Killeen, Zeming Lin, Natalia Gimelshein, Luca Antiga, et al. Pytorch: an imperative style, high-performance deep learning library. In *NeurIPS*, 2019. 6
- [66] Mark Sandler, Andrew Howard, Menglong Zhu, Andrey Zhmoginov, and Liang-Chieh Chen. Mobilenetv2: Inverted residuals and linear bottlenecks. In *CVPR*, 2018. 3
- [67] Jonas Schult, Francis Engelmann, Alexander Hermans, Or Litany, Siyu Tang, and Bastian Leibe. Mask3D: Mask Transformer for 3D Semantic Instance Segmentation. *ICRA*, 2023. 2
- [68] Peize Sun, Rufeng Zhang, Yi Jiang, Tao Kong, Chenfeng Xu, Wei Zhan, Masayoshi Tomizuka, Lei Li, Zehuan Yuan, Changhu Wang, and Ping Luo. SparseR-CNN: End-to-end object detection with learnable proposals. *CVPR*, 2021. 5, 7
- [69] Shuyang Sun, Weijun Wang, Qihang Yu, Andrew Howard, Philip Torr, and Liang-Chieh Chen. Remax: Relaxing for better training on efficient panoptic segmentation. *arXiv preprint arXiv:2306.17319*, 2023. 3
- [70] Ashish Vaswani, Noam Shazeer, Niki Parmar, Jakob Uszkoreit, Llion Jones, Aidan N Gomez, Lukasz Kaiser, and Illia Polosukhin. Attention is all you need. In *NIPS*, 2017. 5
- [71] Qiang Wan, Zilong Huang, Jiachen Lu, Gang Yu, and Li Zhang. Seaformer: Squeeze-enhanced axial transformer for mobile semantic segmentation. In *ICLR*, 2023. 3, 4
- [72] Huiyu Wang, Yukun Zhu, Hartwig Adam, Alan Yuille, and Liang-Chieh Chen. Max-deeplab: End-to-end panoptic segmentation with mask transformers. In *CVPR*, 2021. 5
- [73] Xinlong Wang, Tao Kong, Chunhua Shen, Yuning Jiang, and Lei Li. Solo: Segmenting objects by locations. In *ECCV*, 2020. 5
- [74] Xinlong Wang, Wen Wang, Yue Cao, Chunhua Shen, and Tiejun Huang. Images speak in images: A generalist painter for in-context visual learning. In *CVPR*, 2023. 1
- [75] Xinlong Wang, Xiaosong Zhang, Yue Cao, Wen Wang, Chunhua Shen, and Tiejun Huang. Seggpt: Segmenting everything in context. In *ICCV*, 2023. 1, 3
- [76] M. Weber, J. Xie, M. Collins, Yukun Zhu, P. Voigtlaender, H. Adam, B. Green, A. Geiger, B. Leibe, D. Cremers, Aljosa Osep, L. Leal-Taixé, and Liang-Chieh Chen. Step: Segmenting and tracking every pixel. *NeurIPS*, 2021. 6
- [77] Junde Wu, Rao Fu, Huihui Fang, Yuanpei Liu, Zhaowei Wang, Yanwu Xu, Yueming Jin, and Tal Arbel. Medical sam adapter: Adapting segment anything model for medical image segmentation. *arXiv preprint arXiv:2304.12620*, 2023. 3
- [78] Zeqi Xiao, Wenwei Zhang, Tai Wang, Chen Change Loy, Dahua Lin, and Jiangmiao Pang. Position-guided point cloud panoptic segmentation transformer. *arXiv preprint*, 2023. 2
- [79] Shilin Xu, Xiangtai Li, Jingbo Wang, Guangliang Cheng, Yunhai Tong, and Dacheng Tao. Fashionformer: A simple, effective and unified baseline for human fashion segmentation and recognition. *ECCV*, 2022. 2
- [80] Bin Yan, Yi Jiang, Jiannan Wu, Dong Wang, Zehuan Yuan, Ping Luo, and Huchuan Lu. Universal instance perception as object discovery and retrieval. In *CVPR*, 2023. 1, 2
- [81] Linjie Yang, Yuchen Fan, and Ning Xu. Video instance segmentation. In *ICCV*, 2019. 2, 3, 6
- [82] Shusheng Yang, Yuxin Fang, Xinggang Wang, Yu Li, Chen Fang, Ying Shan, Bin Feng, and Wenyu Liu. Crossover learning for fast online video instance segmentation. In *ICCV*, 2021. 3
- [83] Changqian Yu, Changxin Gao, Jingbo Wang, Gang Yu, Chunhua Shen, and Nong Sang. Bisenet v2: Bilateral network with guided aggregation for real-time semantic segmentation. *IJCV*, 2021. 3
- [84] Changqian Yu, Jingbo Wang, Chao Peng, Changxin Gao, Gang Yu, and Nong Sang. Bisenet: Bilateral segmentation network for real-time semantic segmentation. In *ECCV*, 2018. 3, 4
- [85] Qihang Yu, Huiyu Wang, Siyuan Qiao, Maxwell Collins, Yukun Zhu, Hartwig Adam, Alan Yuille, and Liang-Chieh Chen. k-means mask transformer. In *ECCV*, 2022. 2, 6, 9
- [86] Haobo Yuan, Xiangtai Li, Yibo Yang, Guangliang Cheng, Jing Zhang, Yunhai Tong, Lefei Zhang, and Dacheng Tao. Polyphonicformer: Unified query learning for depth-aware video panoptic segmentation. *ECCV*, 2022.
- [87] Haobo Yuan, Xiangtai Li, Chong Zhou, Yining Li, Kai Chen, and Chen Change Loy. Open-vocabulary sam: Segment and recognize twenty-thousand classes interactively. *arXiv preprint*, 2024. 2
- [88] Yuhui Yuan, Xilin Chen, and Jingdong Wang. Object-contextual representations for semantic segmentation. In *ECCV*, 2020. 2
- [89] Chaoning Zhang, Dongshen Han, Yu Qiao, Jung Uk Kim, Sung-Ho Bae, Seungkyu Lee, and Choong Seon Hong. Faster segment anything: Towards lightweight sam for mobile applications. *arXiv preprint arXiv:2306.14289*, 2023. 3
- [90] Jiangning Zhang, Xiangtai Li, Jian Li, Liang Liu, Zhucun Xue, Boshen Zhang, Zhengkai Jiang, Tianxin Huang,

- Yabiao Wang, and Chengjie Wang. Rethinking mobile block for efficient attention-based models. In *ICCV*, 2023. [3](#)
- [91] Renhong Zhang, Tianheng Cheng, Shusheng Yang, Haoyi Jiang, Shuai Zhang, Jiancheng Lyu, Xin Li, Xiaowen Ying, Dashan Gao, Wenyu Liu, et al. Mobileinst: Video instance segmentation on the mobile. *arXiv preprint arXiv:2303.17594*, 2023. [3](#), [4](#)
- [92] Wenqiang Zhang, Zilong Huang, Guozhong Luo, Tao Chen, Xinggang Wang, Wenyu Liu, Gang Yu, and Chunhua Shen. Topformer: Token pyramid transformer for mobile semantic segmentation. In *CVPR*, 2022. [3](#), [6](#)
- [93] Wenwei Zhang, Jiangmiao Pang, Kai Chen, and Chen Change Loy. K-net: Towards unified image segmentation. In *NeurIPS*, 2021. [2](#), [4](#), [5](#), [7](#), [9](#), [10](#)
- [94] Xiangyu Zhang, Xinyu Zhou, Mengxiao Lin, and Jian Sun. Shufflenet: An extremely efficient convolutional neural network for mobile devices. In *CVPR*, 2018. [3](#)
- [95] Hengshuang Zhao, Xiaojuan Qi, Xiaoyong Shen, Jianping Shi, and Jiaya Jia. Icnet for real-time semantic segmentation on high-resolution images. In *ECCV*, 2018. [3](#), [4](#)
- [96] Hengshuang Zhao, Jianping Shi, Xiaojuan Qi, Xiaogang Wang, and Jiaya Jia. Pyramid scene parsing network. In *CVPR*, 2017. [2](#)
- [97] Xu Zhao, Wenchao Ding, Yongqi An, Yinglong Du, Tao Yu, Min Li, Ming Tang, and Jinqiao Wang. Fast segment anything, 2023. [3](#)
- [98] Bolei Zhou, Hang Zhao, Xavier Puig, Sanja Fidler, Adela Barriuso, and Antonio Torralba. Semantic understanding of scenes through the ADE20K dataset. *CVPR*, 2017. [6](#)
- [99] Chong Zhou, Xiangtai Li, Chen Change Loy, and Bo Dai. Edgesam: Prompt-in-the-loop distillation for on-device deployment of sam. *arXiv preprint arXiv:2312.06660*, 2023. [3](#)
- [100] Qianyu Zhou, Xiangtai Li, Lu He, Yibo Yang, Guangliang Cheng, Yunhai Tong, Lizhuang Ma, and Dacheng Tao. Transvod: End-to-end video object detection with spatial-temporal transformers. *TPAMI*, 2022. [3](#)